JOURNAL OF CATALYSIS 46, 402–413 (1977)

Preparation and Characterization of Catalytic Lanthanum Oxide

MICHAEL P. ROSYNEK[1] AND DENISE T. MAGNUSON

Department of Chemistry, Texas A & M University, College Station, Texas 77843

Received August 30, 1976; revised November 29, 1976

Surface parameters and thermal dehydration/rehydration behavior of the $La(OH)_3/La_2O_3$ system have been examined with a view toward establishing suitable methods for preparing and characterizing catalytic forms of the rare earth oxides. Relatively nonporous $La(OH)_3$, prepared by hydrolysis of the pure oxide, undergoes thermal dehydration in two distinct stages. A well-defined oxyhydroxide (LaOOH) intermediate, formed by dehydration of the hydroxide at 200°C, decomposes in a second step at 300°C to generate the sesquioxide. A surface carbonate layer on the resulting oxide is only removed completely by subsequent thermal treatment at 700–800°C. Exposure of the oxide to water vapor at <200°C causes complete rehydration to the trihydroxide, rather than mere formation of surface hydroxyl groups, and results in complete recovery of surface area lost by high-temperature sintering. Spectroscopic studies reveal the existence of two structurally dissimilar kinds of bulk hydroxide ions in $La(OH)_3$, differing in their relative extents of hydrogen bonding and giving rise to infrared bands at 3610 and 3590 cm^{-1}. The latter band corresponds to the less numerous and more strongly bound type of OH^- that is removed during second-stage dehydration of the oxyhydroxide.

INTRODUCTION

Although the fundamental catalytic and surface properties of alkali, alkaline earth, and other basic oxides have been extensively studied and documented (*1*), equivalent information about the series of basic rare earth oxides is fragmentary. This family of refractories resembles the alkaline earth oxides in many respects, but offers a unique opportunity to study the effects of smoothly varying periodic trends on catalytic behavior. In particular, the gradual decrease in tervalent ionic radius, and consequent increase in ionic charge density, in going from La^{3+} (1.06 Å) to Lu^{3+} (0.85 Å) results in a corresponding decrease in basicity of the sesquioxides (M_2O_3) across the series (*2*). Furthermore, with only few irregularities, the effects of this basicity trend on catalytic properties can be assessed independently of other electronic and solid-state parameters, such as *d*-electron configuration, crystal structure, and preferred stoichiometry, which are largely invariant throughout the oxide series. All Ln^{3+} ions, for example, lack *5d* electrons and differ from each other electronically only in respective configurations of highly shielded *4f* electrons. Systematic correlations, however, between surface basicity and catalytic properties among the rare earth oxides have been explored to only a limited extent.

Empirical studies have demonstrated that, following appropriate pretreatment, rare earth sesquioxides are active catalysts for a variety of reactions, including *ortho/para*-hydrogen conversion (*3*), deuterium exchange reactions of hydrocarbons (*4*), H_2–D_2 equilibration (*5*), alcohol dehydration (*6*), olefin isomerization (*7*), decompositions of N_2O and NO (*8*, *9*), and oxidation reactions of hydrogen (*10*),

[1] To whom all correspondence should be addressed.

ISSN 0021-9517

carbon monoxide (*11*), and hydrocarbons (*12*, *13*). With few exceptions, however, these studies have been primarily exploratory in nature, with the aim of obtaining kinetic data for the reactions investigated and comparative activity levels for the various oxides. Relatively little effort, on the other hand, has been devoted to elucidating the fundamental characteristics of rare earth oxide surfaces. Information is sparse, for example, about the structures, chemical natures, and surface densities of both catalytic and adsorption sites on these materials, and about the modes of interaction of such sites with adsorbed and/or reacting species (*14*, *15*). In addition, apart from the work of Tosun and Rase (*16*), few attempts have been made to characterize in detail the thermal processes by which catalytically active and reproducible forms of the oxides may be prepared.

In beginning a systematic investigation of the fundamental catalytic and surface properties of these materials, therefore, we have applied several physical and instrumental techniques in an effort to establish optimum conditions of oxide preparation, and to define more precisely the dehydration/rehydration behavior and physical parameters of rare earth oxide catalysts and their precursors. The present paper reports such characterization data for the lanthanum oxide/hydroxide system. It should be recognized, however, that certain of the results described may not be representative of the behaviors of other rare earth oxides since La_2O_3, although it is the commonest and most widely studied of the lanthanide oxides, is also the most atypical. It is the most ionic and most highly basic member of the group and, apart from Nd_2O_3 and Ce_2O_3 (which is prepared only with difficulty by reduction of CeO_2), is the only sesquioxide of the series that invariably exists in the type-A (hexagonal) crystal structure, the others being of the type-C (body-centered cubic) structure at $<900°C$ (*17*). Moreover, the electronic and magnetic properties of La_2O_3 differ considerably from those of the other oxides in the series because La^{3+} is the only tervalent rare earth cation that lacks $4f$ electrons and has the simple [Xe] electronic structure.

EXPERIMENTAL METHODS

Materials. Lanthanum trihydroxide, $La(OH)_3$, when precipitated with aqueous ammonia from solutions of the corresponding nitrate, chloride, or sulfate, invariably occludes large amounts of these anions which cannot be removed even by extensive washing, and which drastically affect both the decomposition profile of the hydroxide and the catalytic and surface properties of the resulting oxide. This effect is observed with all Ln^{3+} solutions, including those of Sc^{3+} and Y^{3+}, and has recently been established on a quantitative basis (*18*). In the present study, $La(OH)_3$ was prepared by hydrolyzing La_2O_3 (Ventron Corp., 99.9%), having a surface area of <0.2 m^2/g, in an excess of deionized, triply distilled water for 16 hr at 80°C, followed by filtration, overnight drying at 100°C, and appropriate sizing. This procedure results in complete conversion to the trihydroxide and yields a product having a considerably larger surface area and smaller particle size than the original oxide starting material (*vide infra*).

Nitrogen was Airco pre-purified grade (99.998%) and was further dried before use by passage through a trap containing Linde 5A molecular sieve adsorbent at $-196°C$. Carbon dioxide was Matheson Co. instrument grade (99.99%) and was passed through a trap at $-78°C$ before use. H_2O and D_2O (Bio-Rad Co., 99.8 mole% D) were freed of carbon dioxide by boiling for 1 hr at atmospheric pressure, followed by four distillations from 25 to $-78°C$ and evacuation at the latter temperature each time to a residual pressure of $<10^{-3}$ Torr.

Apparatus. Thermogravimetric analyses, surface area determinations, and quantita-

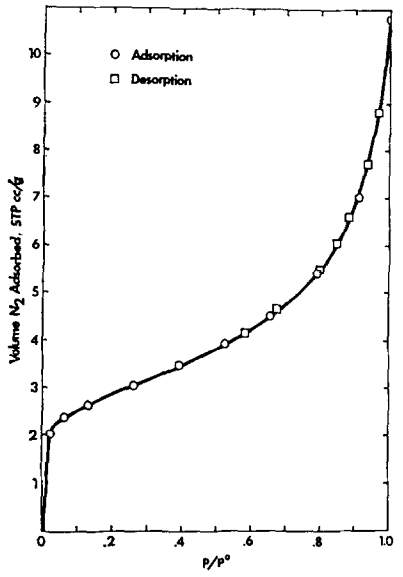

FIG. 1. Nitrogen adsorption/desorption isotherm on prepared $La(OH)_3$ at −196°C.

tive weight change studies were made with a Cahn Model RG recording electrobalance, equipped with a Model 3100 time derivative computer, linear temperature programmer, and quartz sample enclosure tube. The balance chamber was evacuable by a conventional diffusion-pumped, high vacuum gas handling system. Pressures were measured with calibrated McLeod and thermocouple gauges and mercury manometer, and a pressure of 10^{-5} Torr could be routinely achieved in the balance vessel. Isothermal temperature control to ±0.5°C was attained with a digital proportional band controller. Hydroxide samples for the various gravimetric measurements were in the form of irregular 20–30 mesh granules.

Differential thermal analyses were made with a Columbia Scientific Industries Model DTA 500 instrument, comprising a Model P 500 temperature programmer and A 501 amplifier. Powdered samples were contained in platinum pans resting on ring-type differential thermocouples. The reference material for all DTA runs was α-alumina that had been previously calcined in air for 8 hr at 1000°C.

X-Ray diffraction patterns of powdered samples were obtained using a Phillips-Norelco film unit having a camera radius of 2.87 cm. Line intensities were qualitatively estimated. Scanning electron micrographs were obtained from a Joel Model JSM-25 unit operated at an accelerating voltage of 15 kV. Plates for microscopic studies were prepared by spreading with a petroleum ether dispersion of powdered sample, followed by solvent evaporation and drying at 100°C. Pore volume distributions were determined with an American Instrument Co. Model 5-7125B mercury porosimeter having a lower pore size detection limit of 29 Å. Mass spectral analyses were made with an Electronic Associates, Inc. Model 1200 quadrupole-type residual gas analyzer at an ionizing voltage of 70 eV.

Infrared spectra of pressed sample discs were recorded with a Beckman Model IR-9 spectrophotometer, with spectral slit width adjusted to give resolutions of 1.5 and 5.0 cm^{-1} at 1200 and 3000 cm^{-1}, respectively. All samples had an optical density of 10 mg/cm^2 (dehydrated weight), and were prepared by compressing the finely powdered trihydroxide at 900 kg/cm^2 between hardened steel blocks. Dehydration to the oxide was performed *in situ* in a high vacuum quartz cell of conventional design (*19*). A windlass arrangement with plati-

TABLE 1

Pore Volume Distributions of La_2O_3 Starting Material and Prepared La(OH)

Pore diam (μm)	Total pore vol (%)	
	La_2O	$La(OH)_3$
<0.01	2	1
0.01–0.05	3	3
0.05–0.1	2	4
0.1–0.5	18	43
0.5–1	31	5
1–5	23	6
5–10	8	3
10–50	12	34
>50	1	1

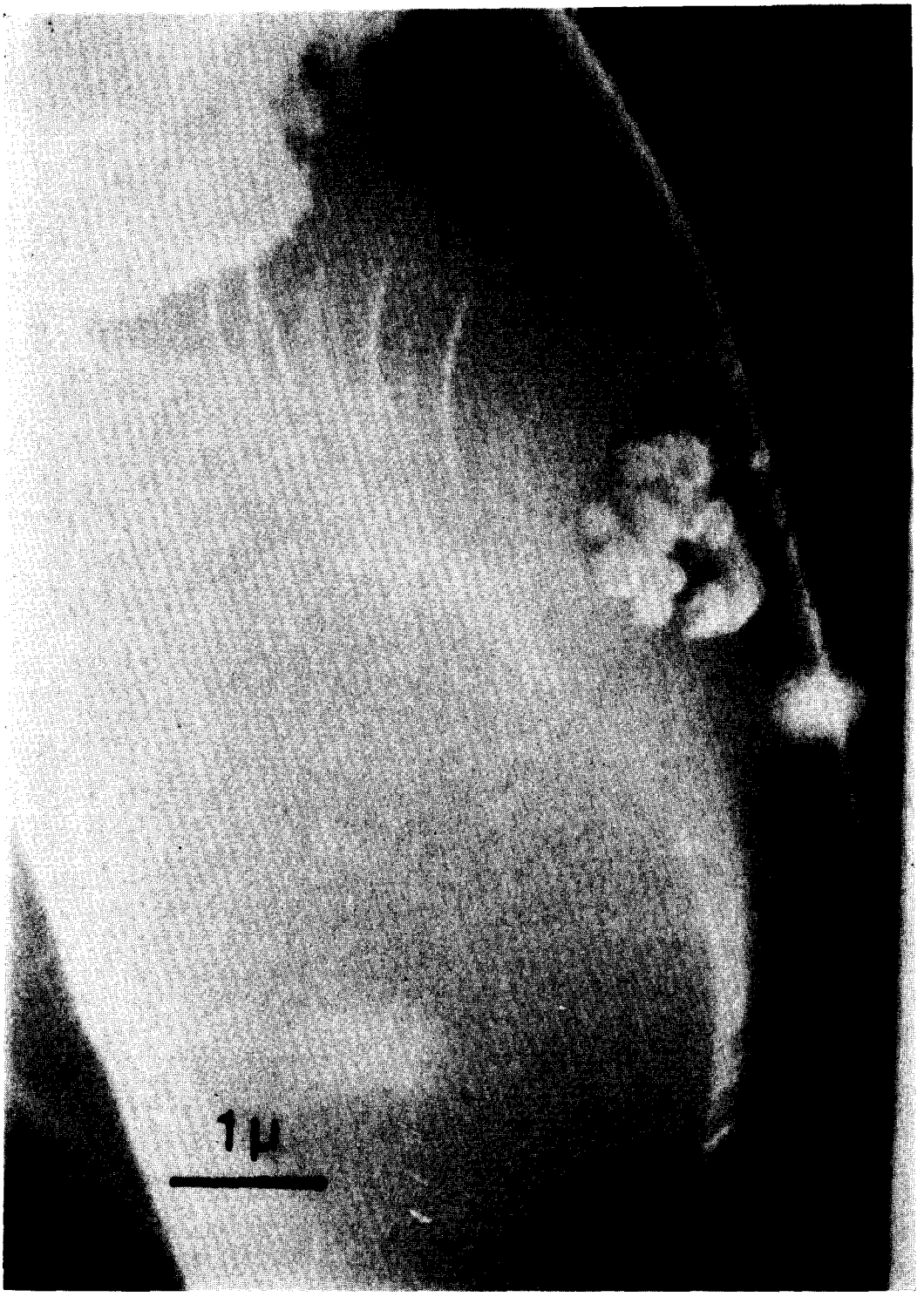

FIG. 2. Scanning electron micrograph of La_2O_3 starting material.

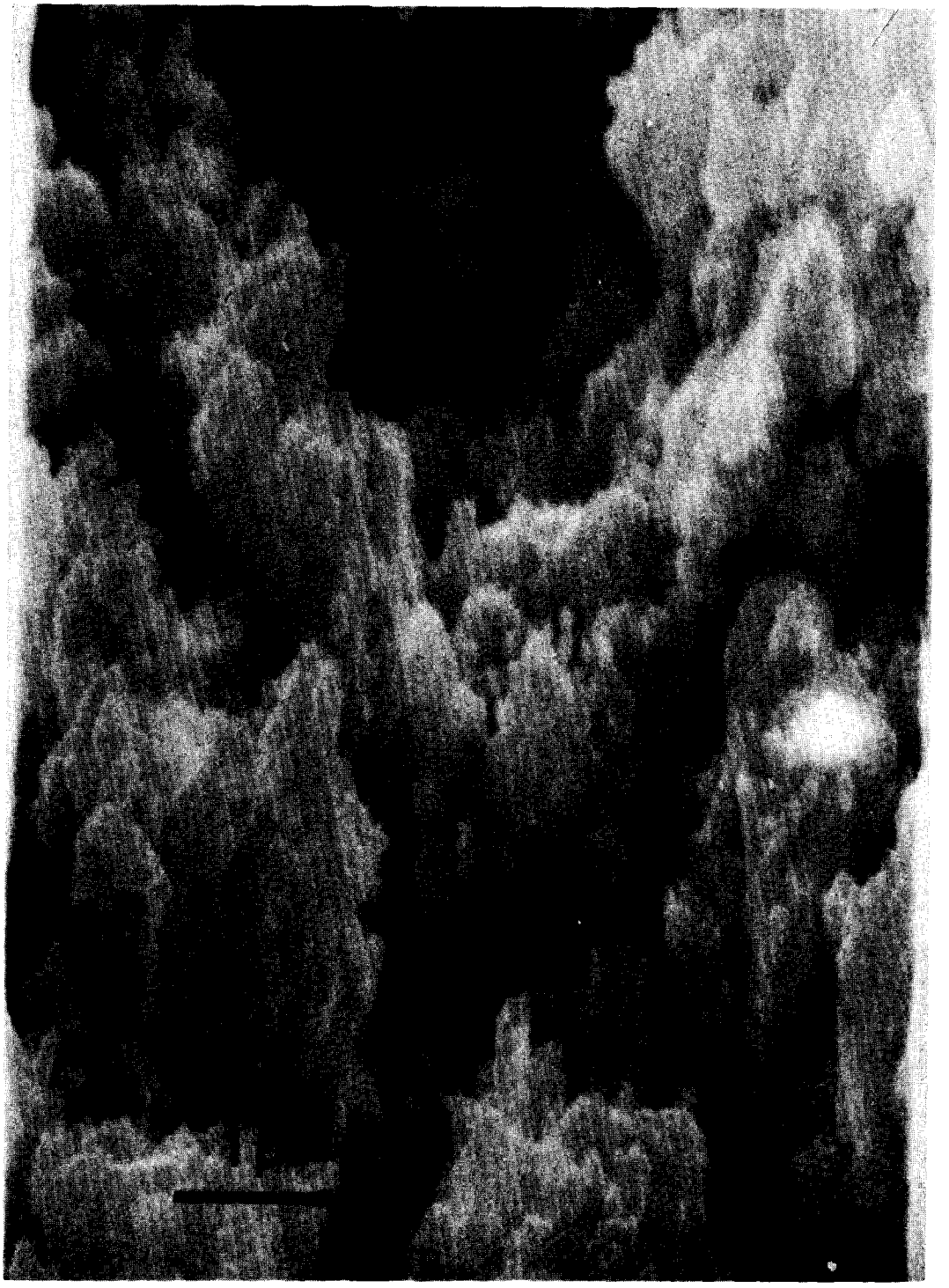

FIG. 3. Scanning electron micrograph of prepared $La(OH)_3$.

num suspension wire was used to position a quartz holder with vertically mounted sample disc in either a thermostatically controlled region for heat treatment or between sealed KCl windows for spectral measurements. Total interior path length between the windows was 1.0 cm, and all spectra were recorded in the double-beam mode, using air as a reference, with the sample at room temperature.

RESULTS AND DISCUSSION

Physical characterization of prepared $La(OH)_3$. Lanthanum trihydroxide, prepared as described above, had a BET-N_2 surface area of 11.0 ± 0.5 m^2/g. A complete N_2 adsorption isotherm, obtained at −196°C, is shown in Fig. 1. The isotherm lacks evidence of both capillary condensation and desorption hysteresis and is characteristic of macro- or nonporous, low surface area materials (*20*). Final N_2 uptake at $P/P_0 = 1$ corresponded to a minimum total pore volume of 0.017 cm^3/g. Except for different absolute adsorption levels due to lower surface areas, qualitatively similar isotherms were obtained for the sesquioxide that resulted from thermal decomposition of $La(OH)_3$.

The lack of generation of a well-developed micro- or mesopore system during hydroxide preparation was confirmed by mercury porosimetry measurements, which are compared in Table 1 for the original La_2O_3 starting material and the resulting trihydroxide. The pore volume distribution in the prepared $La(OH)_3$ was very broad and largely bimodal, with almost 80% of the total pore volume contributed by pores in the two size ranges 10–50 and 0.1–0.5 μm, and only 8% by pores smaller than 0.1 μm (1000 Å) in diameter. The available surface area of the hydroxide (and subsequently formed oxide) can thus be considered as primarily geometric and due to relatively large pores and irregularities on the particle surfaces.

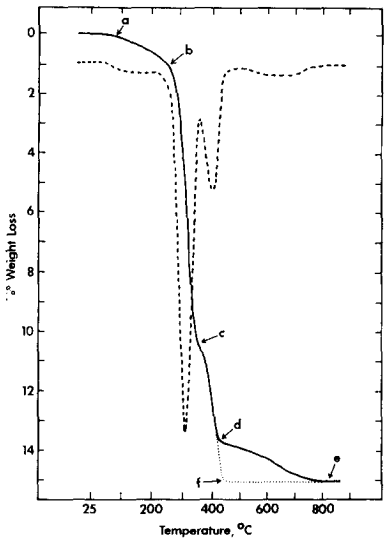

FIG. 4. Thermogram of prepared $La(OH)_3$ at 2°C/min in vacuum. (——) Integral weight loss curve; (— —) time/temperature derivative; (...) pathway followed by rehydrated La_2O_3 sample during second stage of dehydration.

Typical scanning electron micrographs at identical magnifications (~10,000×) are shown in Figs. 2 and 3 for the original oxide and final trihydroxide, respectively. The reduction in particle size effected by the hydrolysis procedure and the extent of surface irregularity in the hydroxide are evident.

Dehydration/rehydration behavior of $La(OH)_3/La_2O_3$. Lanthanum trihydroxide decomposes into the corresponding sesquioxide by passing through an oxyhydroxide (LaOOH) intermediate. If the decomposition is performed in vacuum rather than in air, exposure of the resulting oxide to excess water vapor at <200°C causes complete rehydration to the trihydroxide, rather than mere formation of surface hydroxyl groups, as occurs with more covalently bonded oxides such as silica and alumina.

A typical TGA trace obtained for the prepared $La(OH)_3$ at a heating rate of 2°C/min in vacuum is shown by the solid curve in Fig. 4; its time/temperature

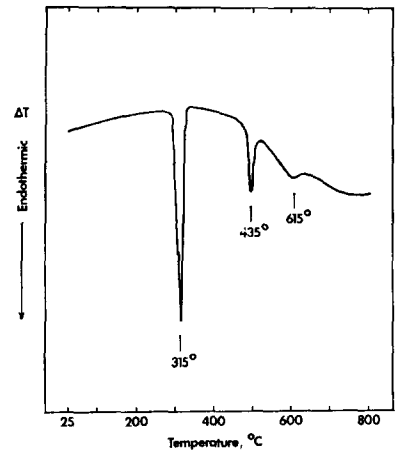

FIG. 5. Differential thermogram of prepared $La(OH)_3$ at 2°C/min in air.

derivative is represented by the broken curve. The initial 0.7% weight decrease that occurs at 100–250°C (a–b) is due to loss of adsorbed water and/or water of crystallization. At the heating rate employed, the first true stage of $La(OH)_3$ decomposition occurs in the temperature range 250–350°C and results in the formation of a well-defined LaOOH intermediate, represented by the break in the integral TGA curve at point c. Subsequent dehydration of the oxyhydroxide to La_2O_3 occurs at 350–420°C (c–d) and is complete at the latter temperature.

The final broad weight loss that occurs in the temperature range 450–800°C (d–e) is due to decomposition of a carbonate layer that invariably exists on the oxide surface as a result of interaction of the highly basic trihydroxide precursor with atmospheric carbon dioxide during preparation and handling:

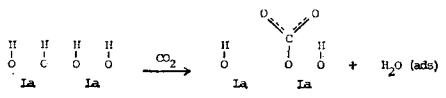

(1)

This surface carbonation process results in a loss of certain hydroxide ions from the $La(OH)_3$ lattice, and causes the weight loss accompanying the second stage of dehydration (c–d) to be lower than the expected value, viz, one-half that of the first-stage decrease (b–c).

Although various workers have previously ascribed the high-temperature weight loss observed during $La(OH)_3$ dehydration to a multistep decomposition of LaOOH (*21*), a carbonate decomposition processes is a more likely explanation of this phenomenon. Effluent gas collected while the TGA run of Fig. 4 was in the temperature range 500–800°C was devoid of H_2O and consisted almost entirely of CO_2, as confirmed by mass spectral analyses. Furthermore, when an La_2O_3 sample which had been evacuated for 6 hr at 800°C following a TGA experiment was rehydrated with gaseous, CO_2-free H_2O at 25°C and the programmed decomposition repeated, the final stage of dehydration followed the pathway indicated by the dotted curve (d–f–e) in Fig. 4. The incremental weight losses of 9.50% (b–c) and 4.75% (c–f) observed in this case were in close agreement with the expected values (9.48 and 4.74%) for $La(OH)_3$ dehydration. Exposure of an identically rehydrated La_2O_3 sample, on the other hand, to 50 Torr of dry CO_2 for 6 hr at 25°C prior to dehydration regenerated the original solid curve of Fig. 4. In addition, infrared spectra of the prepared $La(OH)_3$ recorded prior to thermal treatment exhibited an intense doublet at 1400–1500 cm^{-1}, attributable to the doubly degenerate asymmetric stretching mode of a uni-dentate carbonate entity, which could only be completely removed by evacuation at >700°C. Additional details of the interaction of CO_2 with the La_2O_3/LaOOH/$La(OH)_3$ system are described elsewhere (*22*).

Differential thermal analyses (Fig. 5) qualitatively confirmed the expected endothermic natures of the dehydration and carbonate decomposition processes. Peak maxima in the DTA runs occurred at somewhat higher temperatures than their counterparts in the TGA studies because

the former decompositions were performed in air rather than in vacuum. The small partial pressure of atmospheric H_2O slightly impedes the dehydration stages.

Although TGA and DTA studies provide useful profiles of the overall decomposition process, the dynamic heating methods employed in these techniques do not represent conditions of true thermal equilibrium. At the limit of zero heating rate, the various stages of dehydration are initiated at considerably lower temperatures than those observed at the relatively high program rates described above. Additional dehydration data were therefore obtained for a single sample of the prepared $La(OH)_3$ by separate evacuations of 40 hr at each of a series of increasing temperatures; these are summarized in Table 2. Sample phases were identified by comparing X-ray powder patterns of identically treated aliquots with previously reported standards (*23–25*). The type-A (hexagonal) modification of La_2O_3 was obtained as the final decomposition product in all cases. It is apparent that prolonged evacuation at 200°C is sufficient to cause first-stage dehydration of $La(OH)_3$ to LaOOH, and that subsequent dehydration to the sesquioxide is complete at 300–400°C. The remaining incremental weight losses that occur at 400–800°C are due to decomposition of the surface carbonate layer. Identical results were obtained with rehydrated La_2O_3 samples, except that the cumulative weight loss above 400°C was only 0.05%.

Representative variations in BET-N_2 surface areas (normalized to La_2O_3 content) with calcination temperature are compared in Table 3 for the originally prepared $La(OH)_3$ and for a rehydrated sample. The latter was prepared by evacuating an La_2O_3 sample for 16 hr at 800°C to eliminate the surface carbonate layer, cooling at 10°C/min in 20 Torr of CO_2-free H_2O to 25°C, maintaining 3 hr at the latter temperature, and finally evacuating for 16 hr at 100°C.

TABLE 2

Isothermal Decomposition Behavior of Prepared $La(OH)_3$

Evacuation temp (°C)[a]	Cumulative % wt loss	Phase(s) present
25	0.00	$La(OH)_3$
100	0.66	$La(OH)_3$
150	1.56	$La(OH)_3$ + LaOOH (tr.)
200	10.27	LaOOH
300	13.87	La_2O_3 + LaOOH (tr.)
400	14.13	La_2O_3
500	14.41	La_2O_3
600	14.80	La_2O_3
700	14.93	La_2O_3
800	14.96	La_2O_3

[a] Evacuation for 40 hr at each temperature.

For both the original and rehydrated $La(OH)_3$ samples, the two stages of dehydration that occur at 200 and 300°C cause small decreases in surface area due primarily to particle size shrinkage, after which little further change occurs up to ~500°C. The decline in surface area at temperatures >500°C is due to partial sintering of the macropore structure and "annealing" of surface irregularities. Extended calcination (100 hr) at 800°C causes a further, gradual surface area decrease beyond that shown in Table 3.

Consistent with the observed lack of micropore structure in the prepared $La(OH)_3$, rehydration of the La_2O_3 decomposition end product results in a complete recovery of surface area, but to a value even higher than that of the original $La(OH)_3$. The reason for the latter unusual behavior is unclear but is apparently related to the exclusion of CO_2 during the rehydration process, since six subsequent rehydration/dehydration cycles with the same sample gave results identical to those in the third column of Table 3.

Spectral features of $La(OH)_3$ dehydration. Additional details related to the nature of $La(OH)_3$ and its dehydration process were

TABLE 3

Dependence of Surface Area on Calcination Temperature for Prepared $La(OH)_3$ and Rehydrated La_2O_3

Evacuation temp (°C)	Surface area (m^2/g La_2O_3)	
	Prepared $La(OH)_3$	Rehydrated La_2O_3
100	13.9	19.0
200	12.3	16.3
300	11.7	14.5
400	11.8	14.6
500	11.7	13.6
600	10.1	12.1
700	8.4	10.4
800	6.8	7.9

obtained by examining infrared spectra of pressed samples at various stages of decomposition. A dehydrated La_2O_3 disc was rehydrated as described above, and then evacuated for 6 hr at each of several temperatures in the range 25–300°C, a spectrum being recorded after each temperature increment. The resulting spectra are shown for the O–H stretching and deformation regions in Fig. 6.

The weak band in the spectrum of $La(OH)_3$ at 3460 cm^{-1} is due to the O–H stretching mode of adsorbed water and/or water of crystallization, and is completely removed by evacuation at 150–175°C, in agreement with the quantitative results presented in Table 2. The closely spaced bands that appear at 3590 and 3610 cm^{-1} represent the O–H stretch of bulk hydroxide ions and indicate the existence of two distinct kinds of such species in $La(OH)_3$. The structural dissimilarity between the two types of ions is manifested, at least in part, by differences in their extents of hydrogen-bonding with neighboring groups in the layered, hexagonal structure of the trihydroxide (*26*), and causes the characteristic two-step dehydration behavior of this material. As evidenced by the thermally induced spectral changes in Fig. 6, the more loosely bound type of OH^- corresponds to the band at 3610 cm^{-1} and is preferentially removed during first-stage dehydration to the oxyhydroxide at 200°C. The other, less numerous, type is extensively hydrogen-bonded, as shown by the breadth of the single 3590 cm^{-1} band that remains following evacuation at 200°C, and is subsequently lost during final dehydration of LaOOH to the sesquioxide at 300°C. (Deviation from the expected 2:1 intensity ratio of the 3610 and 3590 cm^{-1} bands in the $La(OH)_3$ spectrum is a result of the anomalous effect of hydrogen-

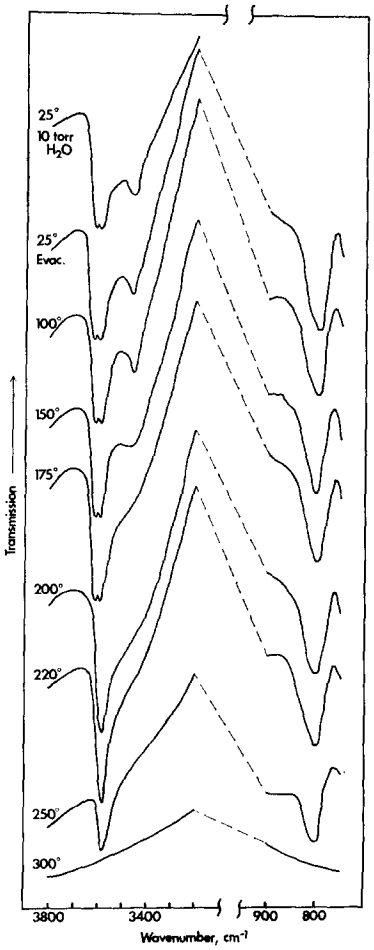

FIG. 6. Infrared spectra of $La(OH)_3$ at various stages of dehydration. Sample prepared by rehydrating La_2O_3 with 10 Torr of H_2O for 3 hr at 25°C, and then evacuating for 6 hr at each of the indicated temperatures (°C).

bonding on the extinction coefficient of the lower frequency band.) Above 300°C, no spectral evidence remained for either bulk or surface hydroxyls in any of the La_2O_3 samples investigated.

Further support of these band assignments was obtained by observing spectral changes caused by exposing an $La(OH)_3$ sample to 50 Torr of CO_2 for 6 hr at 25°C. In addition to the appearance of bands at 1490, 1390, 1060, and 850 cm^{-1} characteristic of a uni-dentate CO_3^{2-} entity, the intensity of the O–H band at 3590 cm^{-1} was markedly reduced, while that of the 3610 cm^{-1} band was virtually unaffected. This result is consistent with the previously discussed TGA profile of the prepared $La(OH)_3$ (Fig. 2) whose appearance in the region c–d–e indicated that the type of OH^- removed during interaction with CO_2 via Eq. (1) is the more strongly bound variety, i.e., that corresponding to the O–H band at 3590 cm^{-1}.

Analogous spectral results were observed with $La(OD)_3$ (Fig. 7), obtained by "rehydration" of La_2O_3 with D_2O. The weak band due to adsorbed D_2O appeared at 2560 cm^{-1}, and the two bulk O–D bands at 2660 and 2670 cm^{-1}. The latter was again removed first, corresponding to LaOOD formation at 200°C, followed by disappearance of the 2660 cm^{-1} band at 300°C. Proton exchange in the trihydroxide is extremely rapid, even at room temperature. Exposure of an evacuated $La(OH)_3$ sample to excess, gaseous D_2O at 25°C causes an almost immediate disappearance of O–H stretching bands and simultaneous appearance of O–D bands. Similarly, rehydration of La_2O_3 with gaseous H_2O/D_2O mixtures generates bands of proportionately diminished intensities in both the O–H and O–D regions of the spectrum.

Because of a broad band due to La–O interactions that occurs in the spectrum of La_2O_3 at 900 cm^{-1}, the 700-1000 cm^{-1} frequency ranges of the spectra shown in Fig. 6 were obtained by digitizing the actual spectra and subtracting from an La_2O_3 background to permit a realistic presentation of spectral features in this region. The band at 800 cm^{-1} in the spectrum of $La(OH)_3$ is due to an La–O–H bending mode, as evidenced by its shift to 650 cm^{-1} in the spectrum of $La(OD)_3$. The intensity of this band appears unaffected

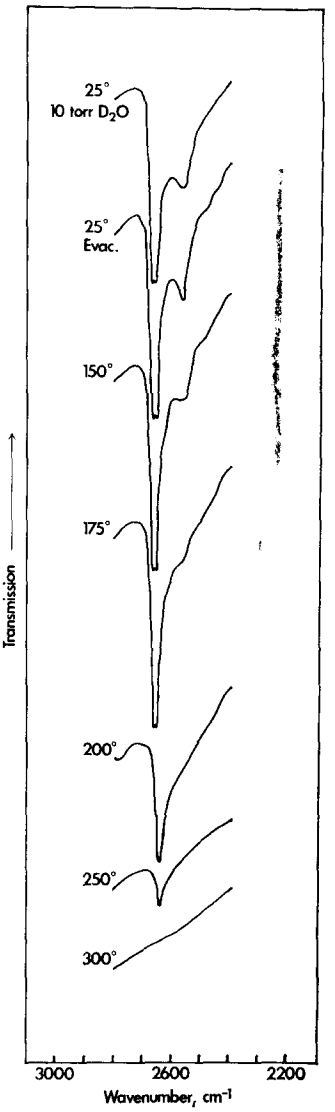

FIG. 7. Infrared spectra of $La(OD)_3$ at various stages of dehydration. Sample prepared by rehydrating La_2O_3 with 10 Torr of D_2O for 3 hr at 25°C, and then evacuating for 6 hr at each of the indicated temperatures (°C).

by first-stage dehydration to the oxyhydroxide, and is evidently associated with the type of OH^- having its stretching frequency at 3590 cm^{-1}. The two bands decrease simultaneously during final dehydration of LaOOH to La_2O_3, and both disappear completely at 300°C.

Application to catalytic studies. The characterization studies described here provide useful indications of suitable methods for preparing lanthanum oxide having the most favorable catalytic and surface properties, and may be applicable in a broader sense to rare earth oxides in general. Because of the marked anion occlusion tendency of precipitated rare earth hydroxides, $La(OH)_3$ formation by hydrolysis of commercially available, low surface area La_2O_3 is preferable to precipitation by aqueous ammonia from nitrate or halide solutions. An alternative, direct route to the oxide is by thermal decomposition of the recrystallized nitrate, but the catalytic properties of the resulting oxide tend to be irreproducible and its surface area is generally lower than that obtained by the hydrolysis method.

Consistent with results of the thermal and spectral studies presented above, lanthanum hydroxide (or "hydrated oxide") has been reported in various previous investigations (*6*, *27*) to be catalytically inactive unless calcined at $\geq$400°C. Above this temperature, dehydration of the oxyhydroxide is complete, and exposed La^{3+} and/or basic O^{2-} ions in various normal or defective surface environments become available for participation as components of "active sites." However, complete removal of the inevitable carbonate layer, which persists on La_2O_3 surfaces long after hydroxide decomposition has been concluded, is also essential if maximum catalytic activity of this material is to be attained. Blockage of basic O^{2-} sites on La_2O_3 by incompletely removed CO_3^{2-} partially inhibits, for example, *n*-butene isomerization on this oxide (*28*), in a manner similar to that observed with alkaline earth oxides (*29*).

The considerable surface area decrease caused by carbonate removal at 800°C (Table 3) can be completely recovered by subsequent rehydration of the oxide with CO_2-free H_2O at <200°C, followed by vacuum calcination at $\geq$300°C. We have used this method, including a brief O_2 treatment at 800°C prior to rehydration, to prepare La_2O_3 having very reproducible surface characteristics and catalytic behavior for low-temperature (0–50°C) *n*-butene isomerization, for which activity of the oxide begins to appear following evacuation at 300°C. With the original, nonrehydrated $La(OH)_3$, on the other hand, calcination at 500°C is required before measurable activity is obtained, due to unremoved surface CO_3^{2-}, and the maximum activity attainable is less than 50% that of a rehydrated catalyst.

ACKNOWLEDGMENTS

We are pleased to acknowledge financial support of this research by the Robert A. Welch Foundation under Grant No. A-619. Thanks are also due to Dr. Walter Henslee of Dow Chemical Co., Freeport, Texas, who performed the mercury porosimetry measurements.

REFERENCES

1. Tanabe, K., "Solid Acids and Bases." Academic Press, New York, 1970.
2. Moeller, T., "The Chemistry of the Lanthanides." Pergamon, New York, 1973.
3. Selwood, P. W., *J. Catal.* **22**, 123 (1971).
4. Minachev, K. M., Vakk, E. G., Dmitriev, R. V., and Nasedkin, E. A., *Izv. Akad. Nauk SSSR, Ser. Khim.*, No. **3**, 421 (1964).
5. Ashmead, D. R., Eley, D. D., and Rudham, R., *J. Catal.* **3**, 280 (1964).
6. Minachev, K. M., *in* "Catalysis" (J. W. Hightower, Ed.), p. 219. North-Holland, Amsterdam, 1973.
7. Khodakov, Y. S., Nesterov, V. K., and Minachev, K. M., *Izv. Akad. Nauk SSSR, Ser. Khim. No.* **9**, 2012 (1975).
8. Read, J. F., *J. Catal.* **28**, 428 (1973).
9. Winter, E. R. S., *J. Catal.* **22**, 158 (1971).

10. Read, J. F., and Conrad, R. E., *J. Phys. Chem.* **76**, 2199 (1972).
11. Artamonov, E. V., and Sazonov, L. A., *Kinet. Katal.* **12**, 961 (1971).
12. Minachev, K. M., Kondrat'ev, D. A., and Antoshin, G. V., *Kinet. Katal.* **8**, 131 (1967).
13. Hattori, H., Inoko, J., and Murakami, Y., *J. Catal.* **42**, 60 (1976).
14. Anderson, J. S., and Gallagher, K. J., *J. Chem. Soc.* 52 (1963).
15. Topchieva, K. V., Loginov, A. Y., and Kreisberg, V. A., *Sovrem. Probl. Fiz. Khim.* **8**, 268 (1975).
16. Tosun, G., and Rase, H. F., *Ind. Eng. Chem. Process Res. Dev.* **11**, 249 (1972).
17. Warshaw, I., and Roy, R., *J. Phys. Chem.* **65**, 2048 (1961).
18. Musorin, V. A., Sakharov, V. V., and Zaitsev, L. M., *Zh. Neorg. Khim.* **19**, 1476 (1974).
19. Peri, J. B., and Hannan, R. B., *J. Phys. Chem.* **64**, 1526 (1960).
20. Ponec, V., Knor, Z., and Cerny, S., "Adsorption on Solids." Butterworth, London, 1974.
21. Brekhunets, A. G., Kokot, I. F., Mank, V. V., and Maknosoev, M. V., *Zh. Neorg. Khim.* **14**, 1460 (1969).
22. Rosynek, M. P., and Magnuson, D. T., unpublished data.
23. Fricke, R., and Seitz, A., *Z. Anorg. Chem.* **254**, 107 (1947).
24. Swanson, H. E., Fuyat, R. K., and Ugrinic, G. M., *Nat. Bur. Std. Circ. 539*, **3**, 33 (1954).
25. Solov'eva, A. E., Gavrish, A. M., and Zoz, E. I., *Zh. Neorg. Khim.* **19**, 1446 (1974).
26. Atoji, M., and Williams, D., *J. Chem. Phys.* **31**, 329 (1959).
27. Khodakov, Y. S., Nakhshunov, V. S., and Minachev, K. M., *Kinet. Katal.* **12**, 535 (1971).
28. Rosynek, M. P., and Fox, J. S., unpublished data.
29. Hattori, H., Yoshii, N., and Tanabe, K., *in* "Catalysis" (J. W. Hightower, Ed.), p. 233. North-Holland, Amsterdam, 1973.